Cluster ionization via two-plasmon excitation

G.F. Bertsch[(a)], N. Van Giai[(b)] and N. Vinh Mau[(b)]

[(a)] *Dept. of Physics and Institute for Nuclear Theory, Box 351560*

University of Washington Seattle, WA 98195

[(b))] *Groupe de Physique Théorique*

Institut de Physique Nucléaire, 91406-Orsay Cedex, France

Abstract

We calculate the two-photon ionization of clusters for photon energies near the surface plasmon resonance. The results are expressed in terms of the ionization rate of a double plasmon excitation, which is calculated perturbatively. For the conditions of the experiment by Schlipper et al., [2], we find an ionization rate of the order of 0.05-0.10 fs^{-1}. This rate is used to determine the ionization probability in an external field in terms of the number of photons absorbed and the duration of the field. The probability also depends on the damping rate of the surface plasmon. Agreement with experiment can only be achieved if the plasmon damping is considerably smaller than its observed width in the room-temperature single-photon absorption spectrum.

I. INTRODUCTION

The electromagnetic response of alkali metal clusters shows a very strong surface plasmon resonance [1], but the interactions of the plasmon with other degrees of freedom are not well understood. One interesting question is the nonlinearities associated with multiple plasmon excitations–how weakly do they interact with each other? Some physical processes can be sensitive to nonlinearities; for example ionization may be energetically impossible for

individual plasmons but allowed for states with multiple plasmon excitations and therefore, ionization rates may depend on the degree of nonlinearity. Recently an experiment was reported observing the ionization probability with different photon field durations [2]. The photon energy was such that ionization is energetically possible only if at least two photons are absorbed. In this work we ask whether the observed ionization can be interpreted as electron emission by a two-plasmon state within a simple theory based on the jellium model of the electronic structure. We will use standard many-body perturbation theory, describing the surface plasmon in RPA as a particle-hole excitation. The plasmon description and details of the jellium model are given in Sect. 2 below.

Our calculation may be viewed as a semianalytic approximation to time-dependent local density approximation (TDLDA), in which the electron dynamics is treated entirely by a common potential field. The TDLDA has been well developed for the high-field response of atoms [3–5], and is now being applied to sodium clusters [6]. Unfortunately, the full TDLDA is computationally difficult and rather opaque, in contrast to the perturbative approach that allows important quantities to be calculated directly.

From the point of view of surface plasmon dynamics, a very important quantity is the ionization rate of a two-plasmon excited state. Haberland et al. [2] interpreted their measurements under the assumption that this rate is fast on a time scale of 10 fs, and we wish to see whether that can be justified theoretically. The two-plasmon ionization rate is calculated in Sect. 3. However, the ionization can take place without the mediation of the plasmon. Also, the plasmon can be excited as a virtual state in which case the connection to the two-plasmon decay formula is unclear. We present in Sect. 4 a more general treatment of the ionization process that includes these effects and allows the role of the plasmon to be isolated from other aspects of the ionization process. The important role of plasmon in screening and enhancement of the external field is made explicit in the formulas discussed there.

II. THE ELECTRONIC STRUCTURE MODEL

In this section we discuss the Hamiltonian model and the treatment of the surface plasmon. We will need single-electron wave functions and energies, which we calculate as follows. We first obtained the solution of the self-consistent jellium model using the computer code "jellyrpa" [7]. The jellium background charge is assumed to be uniform in a sphere of radius $R = r_s N^{1/3}$. Here $r_s = 3.93$ a.u. corresponds to density of charge equal to the bulk density of atoms in sodium metal. It is more convenient for recreating the wave functions to work with analytic models of the potential, so we fit the self-consistent jellium potential to a Woods-Saxon shape. Specifically, we take the electron potential to be

$$V(r) = \frac{-V_0}{1 + e^{(r-R_0)/a}} - V_c(r), \tag{1}$$

where $V_c(r)$ is a Coulomb field associated with the positive charge distributed uniformly in the jellium sphere,

$$\begin{aligned} V_c(r) &= \frac{e^2}{r} \ , \quad r > N^{1/3} r_s \\ &= \frac{e^2}{R}\left(\frac{3}{2} - \frac{r^2}{2R^2}\right) \ , \quad r < N^{1/3} r_s \ . \end{aligned} \tag{2}$$

The parameters that fit this potential to the self-consistent one are $V_0 = 5.71$ eV, $R_0 = 10.548$ Å, and $a = 0.635$ Å. The occupied energy levels of this potential are within 0.2 eV of the self-consistent potential, which is certainly within the accuracy of the jellium model. We find that the cluster has an ionization potential of 4.5 eV. Under the conditions of the experiment [2] using photons of 3.1 eV, two photons are required for ionization on energetic ground. The single-electron spectrum is shown in Fig. 1. We use these orbitals and energies in the RPA and ionization calculations.

The RPA surface plasmon might also be calculated numerically with the code "jellyrpa", but in the interests of developing analytic formulas we adopted a more schematic approach. We take the interaction between electrons to have a separable form [8],

$$v(\mathbf{r}, \mathbf{r}') = \kappa \mathbf{f}(\mathbf{r}) \cdot \mathbf{f}(\mathbf{r}') \ , \tag{3}$$

where $\mathbf{f}$ is a three-dimensional vector with components $\mathbf{f}_\mu(\mathbf{r}) \equiv f(r)Y_1^\mu(\hat{r})$. Then the energies of the RPA excitations satisfy the dispersion relation

$$1 = 2\kappa \sum_{ph} \frac{\langle p|\mathbf{f}_\mu|h\rangle^2(\epsilon_p - \epsilon_h)}{\omega^2 - (\epsilon_p - \epsilon_h)^2} \ , \tag{4}$$

where ϵ is a single-particle energy and p, h label particle and hole orbitals. Due to the spherical symmetry, the solutions ω_n of the dispersion relation are independent of μ. The matrix element $\langle n\mu|\mathbf{f}_\mu|0\rangle$ between the ground state and a one-phonon state of energy ω_n is given by

$$\langle n\mu|\mathbf{f}_\mu|0\rangle = \frac{1}{2\kappa}\left(\omega_n \sum_{ph} \frac{\langle p|\mathbf{f}_\mu|h\rangle^2(\epsilon_p - \epsilon_h)}{(\omega_n^2 - (\epsilon_p - \epsilon_h)^2)^2}\right)^{-1/2} \ . \tag{5}$$

We shall particularly require the transition potential $v_{n\mu}$ associated with the creation of the plasmon. This is given by

$$v_{n\mu} = \kappa \mathbf{f}_\mu(\mathbf{r})\langle n\mu|\mathbf{f}_\mu|0\rangle \ . \tag{6}$$

In the spherical jellium model, the surface plasmon can be roughly described taking the interaction of dipole-dipole form. For an excitation along the z-axis, the field is

$$\mathbf{f}_0(\mathbf{r}) = z \ . \tag{7}$$

Assuming that the transition density of the plasmon is concentrated at the surface at radius R, the strength of the interaction is obtained from the multipole expansion of the Coulomb interaction as

$$\kappa_c = \frac{e^2}{R^3} \ . \tag{8}$$

The dispersion relation can then be solved analytically [9] in the limit $\omega >> (\epsilon_p - \epsilon_h)$ making use of the TRK sum rule. The result is the simple Mie surface plasmon formula,

$$\omega_n^2 = \frac{e^2\hbar^2 N}{mR^3} \ . \tag{9}$$

The resulting energy is about 25% higher than the empirical value for sodium clusters, $\omega \approx 2.75$ eV. The RPA can be made to fit this value for $N = 93$ by renormalizing the

coupling strength by $\kappa = 0.52\kappa_c$. However, the transition potential of eq.(6) calculated with eq.(7) is linear in r whereas TDLDA calculations without separable assumption do not yield this behavior, as shown in Fig. 2. A simple improvement over the linear form eq. (7) is the dipole field associated with a charge distribution localized on the surface of the jellium sphere [10]. A surface charge produces a radial field of the form

$$\begin{aligned} f(r) &= r \quad r < R \ , \\ &= \frac{R^3}{r^2} \quad r > R \ . \end{aligned} \tag{10}$$

This is plotted as the dashed line in Fig. 2; it clearly is much closer to the actual TDLDA transition potential. With this choice, the empirical position of the resonance is obtained by using the coupling $\kappa = 0.6\kappa_c$. This is very close to the previous one, showing that the modified form factor has only a small influence on the plasmon properties. We will see that it is much more important in the ionization process.

In the experimental photoabsorption spectrum, the plasmon has a width of about 0.5 eV. This finite width requires theory beyond RPA, which produces only zero-width excitations below the ionization threshold. Since it is not easy to incorporate the other degrees of freedom that are responsible for the width, we will treat the width phenomenologically. In discussing the response in general, it is useful to consider the dynamic polarizability $\alpha(\omega)$. This is given by

$$\alpha(\omega) = \sum_n \frac{2e^2 \langle n|z|0\rangle^2 \omega_n}{\omega_n^2 - (\omega - i\delta)^2} \tag{11}$$

where n labels the true excitations and δ is a small quantity. A simple prescription is to take a single pole for the plasmon, taking into account the finite width by the replacement $\delta \to \Gamma_n/2$ for a width Γ_n.

The imaginary part of α is related directly to the photoabsorption cross section σ by the formula

$$\sigma = 4\pi \frac{\omega}{c} \text{Im } \alpha(\omega). \tag{12}$$

Given Im $\alpha(\omega)$, the real part can then be computed from the Kramers-Kronig relation,

$$\mathrm{Re}\alpha(\omega) = \frac{1}{\pi}\int_0^\infty d\omega' \mathrm{Im}\alpha(\omega')\left(\frac{2\omega'}{\omega^2-\omega'^2}\right). \tag{13}$$

Applying this to the experimental data of ref. [11], we find the imaginary part of α graphed as the solid line in Fig. 3. This is compared with the single-pole approximation with parameters $\omega_n = 2.75$ eV and $\Gamma_n = 0.5$ eV. A modification of the jellium model was proposed in ref. [12] introducing a soft-edged surface in the distribution of the background charge. We also calculated the full RPA response for soft jellium model, calculated using the program "jellyrpa". In this case the empirical width can be reproduced with a smaller external width parameter. The dashed line shows the fit with $\Gamma_n = 0.3$ eV. Both these models give a reasonable but not quantitative description of the data. The soft jellium model has the advantage that the plasmon can be moved to lower frequency without adjusting the coupling strength. However, it predicts too low an ionization potential, which makes it unsuitable for the autoionization calculation.

The corresponding comparison for the real part of α is shown in Fig. (4). Here the theory is quite robust, and we can rather confidently estimate Re α at the energy of interest (3.1 eV) to be about 3000 Å^3.

III. TWO-PLASMON AUTOIONIZATION RATE

The many-body perturbative graphs for M_{ph}, the interaction matrix element between the two-plasmon excitation of the $n\mu$ mode and the final configuration with a hole h and the electron in a continuum state p , is shown in Fig. 5. The labels p', h' stand for particle and hole states, respectively. Algebraically, the matrix element is given by

$$\begin{aligned} M_{ph} &= \sqrt{2}\Big[\sum_{p'}\Big(\frac{\langle h|v_{n\mu}|p'\rangle\langle p'|v_{n\mu}|p\rangle}{\omega_n-\epsilon_{p'}+\epsilon_h}\Big) - \sum_{h'}\Big(\frac{\langle h|v_{n\mu}|h'\rangle\langle h'|v_{n\mu}|p\rangle}{\omega_n-\epsilon_p+\epsilon_{h'}}\Big)\Big] \\ &= \sqrt{2}\sum_{i'}\Big(\frac{\langle h|v_{n\mu}|i'\rangle\langle i'|v_{n\mu}|p\rangle}{\omega_n-\epsilon_{i'}+\epsilon_h}\Big)\,, \end{aligned} \tag{14}$$

where $v_{n\mu}$ is defined in eq. (6). The factor $\sqrt{2}$ accounts for the statistics of the two-plasmon initial state. The two graphs can be combined in one sum over both particles and holes as

shown in the second line, making use of the fact that the matrix element is only required on shell, i.e. with $\epsilon_p - \epsilon_h = 2\omega_n$. The primed indices i' indicate particle or hole orbitals, depending on the direction of the arrow. The ionization width $\Gamma_e = \hbar w_e$, where w_e is the ionization rate, is given by the Golden Rule formula,

$$\begin{aligned}\Gamma_e &= 2\pi \sum_{ph} |M_{ph}|^2 \frac{dn_p}{dE} \delta(2\omega_n - \epsilon_p + \epsilon_h) \\ &= 4\pi\kappa^4 \langle\, n|\mathbf{f}_\mu|0\rangle^4 \sum_{ph} |K_{ph}|^2 \frac{dn_p}{dE} \delta(2\omega_n - \epsilon_p + \epsilon_h)\ . \end{aligned} \tag{15}$$

Here dn_p/dE is the density of states of the continuum electron. We have also separated out the excitation amplitude for a field $\mathbf{f}$,

$$K_{ph} = \sum_{i'} \left(\frac{\langle h|\mathbf{f}_\mu|i'\rangle\langle i'|\mathbf{f}_\mu|p\rangle}{\omega_n - \epsilon_{i'} + \epsilon_h} \right) . \tag{16}$$

The sums in eq. (15) can be reduced in size by making use of the angular momentum symmetry of the orbitals. Labeling the angular momentum quantum numbers l and m, we may express the m-dependence of the matrix elements as

$$\langle p', m_{p'}|\mathbf{f}_\mu|p, m_p\rangle = (-1)^{l_{p'} - m_{p'}} \begin{pmatrix} l_{p'} & 1 & l_p \\ -m_{p'} & \mu & m_p \end{pmatrix} \langle p'||\mathbf{f}||p\rangle\ , \tag{17}$$

where the reduced matrix element $\langle a||\mathbf{f}||b\rangle$ is defined as [13]

$$\langle a||\mathbf{f}||b\rangle = (-1)^{l_a} \sqrt{(2l_a+1)(2l_b+1)} \begin{pmatrix} l_a & 1 & l_b \\ 0 & 0 & 0 \end{pmatrix} \int_0^\infty f(r)\varphi_a(r)\varphi_b(r) r^2 dr \tag{18}$$

in terms of the radial wave functions φ_i. The sum over magnetic quantum numbers $m_{p,h}$ implicit in eq. (15) can be evaluated in terms of a 9-j symbol [14] in which the total angular momentum L carried by the two photons appears. The result is

$$\begin{aligned}\sum_{all\ m} |K_{ph}|^2 = 2 \sum_{ij} &\frac{1}{\omega - (\epsilon_j - \epsilon_h)} \frac{1}{\omega - (\epsilon_i - \epsilon_h)} \langle h||\mathbf{f}||j\rangle\langle j||\mathbf{f}||p\rangle\langle i||\mathbf{f}||h\rangle\langle p||\mathbf{f}||i\rangle \\ &\times \sum_{L=0,2} \hat{L}^2 \begin{pmatrix} 1 & 1 & L \\ 0 & 0 & 0 \end{pmatrix}^2 \begin{Bmatrix} 1 & 1 & L \\ l_j & l_p & 1 \\ l_h & l_i & 1 \end{Bmatrix} .\end{aligned} \tag{19}$$

The factor of 2 arises from the two-fold spin degeneracy of the occupied orbitals. In carrying out the calculation one also has to fix the normalization of the continuum radial wave function. A convenient choice is $r\varphi_p \to \sin(kr+\delta)$ at large r, giving $dn_p/dE = 2m/(\pi k\hbar^2)$.

The results for the autoionization of Na_{93}^+ are given in Table I. We chose the plasmon parameter κ in two different ways, requiring the plasmon resonance energy ω_n to be either at the experimental position of 2.75 eV, or at the energy of the absorbed photons, 3.1 eV. The particle-hole states taken into account in the calculations include electron jumps up to three harmonic oscillator shells. We first discuss the results in the case of undamped excitations ($\delta = 0$ in Table I). The upper half of Table I shows the values obtained using the linear dipole field $\mathbf{f}_0 = z$ (eq. (7)). The resulting widths Γ_e are extremely small for both choices of ω_n, and they would be hard to reconcile with experiment. This led us to reexamine our simplifying assumption about the shape of the separable particle-hole interaction. Since the choice of eq. (10) gives a better transition potential (see fig. 2) we use it from now on instead of eq. (7). As shown in the lower half of Table I, the resulting widths are much larger and they seem to give a possibility to explain the data. Indeed, they correspond to ionization times of the order of 5.5 fs to 7.5 fs which is comparable to the estimated plasmon lifetime of 10 fs [2].

However, the calculated results cannot be considered reliable because they are quite sensitive to the single-particle energies involved in the transition. In eq. (16) several states i' give quite small energy denominators (see Fig. 1) and therefore they yield abnormally large contributions. However, it is not consistent to neglect the damping of the excitations in the perturbative calculation when the energy denominators are small. As we did with the plasmon in Sect. 2, we here add a finite imaginary term δ to the energy denominators of eq. (16). In Fig. 6 we show the dependence of $\sum |K_{ph}|^2$ on δ which is seen to be moderate for δ in the range 0.1 - 0.2 eV. We see that the damping reduces the ionization width by roughly a factor of two when $\delta = 0.1$ eV which seems a reasonable value. Although the dependence on the transition field and on the damping makes the calculation uncertain by a factor of two or so, we at least see that the result is rather insensitive to the particular

model for the plasmon excitation energy. This is nice in that it means that the theoretical uncertainty here is not a hindrance to doing the calculation.

The results correspond to a ionization lifetime τ_e of the two-plasmon state in the range of 5 to 10 fs. This is of the same order of magnitude as the plasmon lifetime which is estimated to be about 10 fs [2]. In the present model the ionization process is not very fast contrarily to the assumption made in the interpretation of ref. [2], but it is fast enough to allow for the ionization process to compete with the plasmon damping.

IV. IONIZATION IN A LASER FIELD

In this section we wish to apply the previous results to ionization in a laser field. Thus, we consider the ionization as a multistep process, in which the photons are first absorbed to make plasmons and then the plasmons interact to eject an electron. A simple physical argument can be made to obtain a formula for the ionization, which we will then justify more formally. Let us define the absorption rate for photons R_ν and the damping width for the plasmon Γ_n. In the steady state the balance between the creation and absorption of plasmons gives a mean number of plasmons $\bar{n}$ satisfying

$$\bar{n} = \frac{\hbar R_\nu}{\Gamma_n} \tag{20}$$

Taking the distribution of numbers as Poissonian, the mean number of pairs is then $\bar{n}^2/2$. The ionization rate R_e is related to the two-plasmon ionization width Γ_e by

$$\begin{aligned} R_e &= \frac{\bar{n}^2}{2} w_e \\ &= \frac{\hbar}{2} \frac{R_\nu^2}{\Gamma_n^2} \Gamma_e \ , \end{aligned} \tag{21}$$

where Γ_e and w_e have been introduced in the preceding section.

A more formal derivation of this formula may be made from the graph of Fig. 5 as follows. We add to the graph matrix elements of the external field between the zero- and one-plasmon states,

$$V_n = \langle n|V_{ext}|0\rangle \ . \tag{22}$$

The plasmon propagator itself can be approximated by $1/(-\omega+\omega_n+i\Gamma_n/2)$ for ω close to ω_n. Then the ionization rate for the graph is given by

$$\begin{aligned} R_e &= \frac{2\pi}{\hbar}\sum_{ph}\Big|\Big(\frac{V_n}{-\omega+\omega_n+i\Gamma_n/2}\Big)^2 M_{ph}\Big|^2 \frac{dn_p}{dE} \\ &= \frac{1}{\hbar}\frac{V_n^4}{((\omega_n-\omega)^2+(\Gamma_n/2)^2)^2}\frac{\Gamma_e}{2} \ . \end{aligned} \tag{23}$$

On the other hand, the photon absorption rate can be calculated as the imaginary part of the self-energy associated with the coupling V_n,

$$\begin{aligned} R_\nu &= \frac{-2}{\hbar}V_n^2 \mathrm{Im}\frac{1}{-\omega+\omega_n+i\Gamma_n/2} \\ &= \frac{1}{\hbar}\frac{V_n^2\Gamma_n}{(\omega_n-\omega)^2+(\Gamma_n/2)^2} \ . \end{aligned} \tag{24}$$

Eq. (21) may now be obtained by combining the last two equations.

For comparing with experiment, it is convenient to express eq. (21) in terms of the number of ionizations per cluster $N_e = R_e T$ and the number of photons absorbed $N_\nu = R_\nu T$, where T is the time duration of the laser pulse. We obtain for N_e

$$\begin{aligned} P_e &\equiv \frac{N_e}{N_\nu^2/2} \\ &= \frac{\hbar}{T}\frac{\Gamma_e}{\Gamma_n^2} \ . \end{aligned} \tag{25}$$

The experiment [2] observed not only ionization but considerable evaporation of atoms from the clusters. We note that atomic motion takes place on a much longer time scale than electronic motion. Most of the evaporated particles are emitted from the cluster after it has reached thermal equilibrium; the statistical evaporation theory gives lifetimes in the nanosecond regime for the conditions of the experiment [15]. This is longer than the fast laser pulse duration (T = 140 fs), so we may think that the Na_{93}^+ cluster remains whole before being ionized. The first line of eq. (25) may be estimated from Fig. 2 of ref. [2]. The broad peak in the middle of the mass spectrum represents ionized clusters and has roughly

1/3 of the area of the Na_{93}^+ peak on the right; thus $N_e \approx 1/3$. The number of photons absorbed is given as $N_\nu \approx 6$. Thus we estimate[1] $P_e \approx 0.014$.

To evaluate the second line of eq. (25) we have the calculated Γ_e from Sect. 3 and the experimental pulse duration T, but we still do not have Γ_n, the damping width of the plasmon. As discussed in Sect. 2, this quantity is beyond the scope of RPA, but an upper bound to Γ_n is given by the empirical photoabsorption spectrum. Taking the values ω_n=2.75 eV and $\Gamma_n = 0.5$ eV the single-pole fit to the plasmon and $\delta = 0.2$ eV in the perturbative energy denominators, we find $P_e = 1.0 \times 10^{-3}$, which is much too small. On the other hand, the experimentally quoted lifetime of the plasmon is 10 fs which corresponds to a considerably smaller value of Γ_n. Adopting this value of Γ_n gives $P_e = 5.8 \times 10^{-2}$. The width Γ_e depends on the particular cluster considered since the energetics of the emitted electrons will change somewhat for different clusters.

V. GENERAL THEORY

The theory in the last section assumed that the energy transfer to the electron was indirect, first producing plasmons which then autoionize. In fact the photon could be absorbed directly on the electron. The direct absorption is implicit in the TDLDA, and can be taken into account as well in the perturbative theory of photon absorption [16]. The general expression for a second-order transition from a state i to f is given by

$$w_{fi} = \frac{2\pi}{\hbar} e^4 \mathcal{E}_0^4 |K_{fi}|^2 \frac{dn_f}{dE} \ . \tag{26}$$

The second order matrix element K_{fi} is similar to eq. (16) with the linear field (7), except the particle orbitals are replaced by many-body states i, i', f:

$$K_{fi} = \sum_{i'} \frac{\langle f|z|i'\rangle\langle i'|z|i\rangle}{\omega - E_{i'} + E_i} \tag{27}$$

---

[1]Fitting more extensive data with a rate equation, the authors of ref. [2] find a somewhat larger probability, $P_e \approx 0.06$

In eq. (26) $\mathcal{E}_0$ is the amplitude of the time-dependent electric dipole field, $\vec{\mathcal{E}}(t) = \mathcal{E}_0\mathbf{z}(e^{-i\omega t} + e^{i\omega t})$. It is related to the laser intensity by $\mathcal{E}_0^2 = 2\pi I\omega/c$. Taking the many-body states as the simple particle-hole configurations, eq. (27) reduces to eq. (16). By itself this would only give the ionization probability of the electron in the external field, i.e. without plasmon effects. The many-body physics is included by considering higher-order perturbations in the wave functions including excitation of the other electrons by the active electron. The result is to replace the external field $\mathcal{E}_0$ in eq. (26) by an effective field such that

$$e\mathcal{E}_{eff}z = e\mathcal{E}_0 z - e\int v(r,r')\Pi(r',r")\mathcal{E}_0 z" d^3r' d^3r" \ , \tag{28}$$

where Π is the response function of the cluster.

To make the connection with the previous approach, we approximate the response by a single pole and use the separable approximation. The effective field becomes

$$\begin{aligned} e\mathcal{E}_{eff}z &= e\mathcal{E}_0 z - e\mathcal{E}_0\kappa z\langle n|z|0\rangle\langle 0|z|n\rangle\Big(\frac{1}{-\omega+\omega_n+i\Gamma_n/2} + \frac{1}{\omega+\omega_n-i\Gamma_n/2}\Big) \\ &= e\mathcal{E}_0 z\Big(1 - \frac{\kappa}{e^2}\alpha(\omega)\Big) \ . \end{aligned} \tag{29}$$

Eq. (23) can now be obtained from eq. (29) by dropping the external field contribution as well as the nonresonant term in the polarizability. In the second line, we express the polarization effects as a multiplicative factor, which can be interpreted as an effective charge

$$e_{eff} = e(1 - \frac{\kappa}{e^2}\alpha(\omega)) \ . \tag{30}$$

We may use this expression to assess the relative importance of the external and induced fields. First note that there is a complete cancelation of the two terms in eq. (30), implying complete screening, if we take $\kappa = \kappa_c$ and $\alpha = R^3$. This last is just the classical polarizability of a conducting sphere, and it may also be derived putting the Mie resonance eq. (9) into the polarizability formula eq. (11).

For the present purposes we assume in eq. (29) $\omega_n = 2.75$ eV and $\kappa = 0.52\kappa_c$ as in Sec. 2. We also take for Γ_n a width corresponding to a lifetime of 10 fs. The result at $\omega = 3.1$ eV is

$$\frac{\kappa}{e^2}\alpha(3.1 \text{ eV}) = -3.3 + i0.3 \tag{31}$$

Thus the plasmon enhances the field approximately by a factor of 4.3, showing that the induced field is indeed dominant. This result is insensitive to Γ_n if it is small, but would decrease if the width were as large as the measured width of the optical absorption peak. In a study of Na_9^+ in the TDLDA, ref. [17] obtained enhancement factors on resonance in the range 5-8, which is the same order of magnitude.

The effect on the ionization rate goes as the fourth power of the field,

$$|1 - \frac{\kappa\alpha(3.1 \text{ eV})}{e^2}|^4 = 320 \ , \tag{32}$$

Finally , we use this result to make an improved calculation of the ionization probability P_e introduced in eq. (25). The number of emitted electrons is calculated as $N_e = w_{fi}T$ where w_{fi} is given by eq. (26) with e replaced by e_{eff}. The number of of pairs of absorbed photons is given by $N_{pair} = (I\sigma T)^2/2$, σ being the photo-absorption cross section. Computing σ from eq. (12) we find $P_e = 1.25 \times 10^{-2}$, a magnitude comparable to that found in the preceding section. However, the cross section corresponding to the polarizability in eq. (31) is much too small at 3.1 eV, as is clear from the width discussion in Sect. 2. On the other hand, if we take the width parameter from empirical single-pole fit, $\Gamma_n = 0.5$ eV, the probability comes out very small, as discussed earlier.

VI. CONCLUSION

In this work, we have derived the theory of cluster ionization by multiple photons of frequency near that of the surface plasmon. The weak coupling between the surface plasmons is the driving interaction for the two-photon ionization process, and a perturbative framework with respect to the ionized electron seems reasonable. The plasmon-induced mechanism can be derived from the general perturbative formula using the higher order contributions associated with the screened interaction. Unfortunately, the formula depends quadratically on the damping rate of the plasmon, which is still not fully understood. The rates obtained for Na_{93}^+ are of the order of tens of femtoseconds, which is the same time scale as other relaxation processes.

We have used the jellium model in the calculations, and it is unclear how realistic the model is. We found that the interaction must be treated more accurately than in the small-r separable approximation, but we have not examined the most sophisticated treatment of the interaction which would include the exchange interaction without approximation. The Landau damping of the Mie resonance is much larger with more realistic interactions [18]. A major problem of the jellium model is that the damping is too small. Ionic scattering (called "interband transitions" in condensed matter physics) would increase the spreading width, and the lack of ionic scattering in the jellium model is in general a serious deficiency. However, in the case of Na clusters the realistic Hamiltonian gives a very similar spectrum to the jellium model [19], giving some credibility to the model. Nevertheless, it would be interesting to see what the effects of the ionic scattering are in the second-order ionization. For small Na clusters, more realistic calculations are becoming available of high field ionization using the TDLDA [20], and it would be interesting to compare.

VII. ACKNOWLEDGMENT

We thank P.G. Reinhard for discussions, and G.B. thanks the IPN at Orsay for its hospitality where this work was done. He is also supported in part by the US Department of Energy under Grant DE-FG-06-90ER40561.

REFERENCES

[1] W.A. de Heer, Rev. Mod. Phys. **65**, 611 (1993).

[2] R. Schlipper, R. Kusche, B. von Issendorff and H. Haberland, Phys. Rev. Lett. **80**, 1194 (1998).

[3] G. Senatore and K.S. Subbaswamy, Phys. Rev. **A 35**, 2440 (1987).

[4] X. Tong and S. Chu, Phys. Rev. **A 57**, 452 (1998).

[5] C.A. Ullrich and E.K.U. Gross, Comm. At. Mol. Phys. **33**, 211 (1997).

[6] C.A. Ullrich, P.G. Reinhard and E. Suraud, J. Phys. **B30**, 5043 (1997).

[7] G.F. Bertsch, Computer Physics Com. **60**, 247 (1990).

[8] A. Bohr and B.R. Mottelson, Nuclear Structure, Vol. II, (Benjamin, Reading, 1975), eq. (6-37).

[9] G.F. Bertsch and R.A. Broglia, Oscillations in Finite Quantum Systems, (Cambridge, New York, 1994), p.86.

[10] K. Yabana and G.F. Bertsch, Z. Phys. **D 32**, 329 (1995).

[11] T. Reiners, et al. Phys. Rev. Lett. **74**, 1558 (1995).

[12] F. Calvayrac, E. Suraud, P.G. Reinhard, Ann. Phys. 254 125 (1997).

[13] A. Bohr and B.R. Mottelson, Nuclear Structure, Vol. I, (Benjamin, New York, 1969) p. 82.

[14] M. Rotenberg, et al., The 3-j and 6-j symbols, (MIT Press, Cambridge MA, 1959), eq. (1.22-24).

[15] G.F. Bertsch, N. Oberhofer, and S. Stringari, Z. Phys. **D 20**, 123 (1991).

[16] H.B. Bebb and A. Gold, Phys. Rev. **143**, 1 (1966).

[17] P.G. Reinhard and E. Suraud, Eur. Phys. J. **D 3**, 175 (1998).

[18] M. Madjet, C. Guet and W.R. Johnson, Phys. Rev. **A 51**, 1327 (1995).

[19] K. Yabana and G.F. Bertsch, Phys. Rev. **B54**, 4484 (1996).

[20] M. Brack, F. Calvayrac, C. Kohl, S. Kuemmel, P.G. Reinhard, E. Suraud, and C.A. Ullrich, submitted to Euro. J. Phys.

TABLES

TABLE I. Two-plasmon ionization widths in Na_{93}^{+}. The upper half and lower half of the table correspond to results calculated with the coupling (7) and (10), respectively. The quantities τ_e are defined in the text.

	$\omega_n = 2.75$ eV, $\kappa = 0.91 \times 10^{-2}$ eV$\mathring{A}^{-2}$			$\omega_n = 3.1$ eV, $\kappa = 1.19 \times 10^{-2}$ eV$\mathring{A}^{-2}$		
δ(eV)	0.	0.1	0.2	0.	0.1	0.2
Γ_e(eV)	9×10^{-4}	5×10^{-4}	4×10^{-4}	8.6×10^{-3}	2.8×10^{-3}	1.7×10^{-3}
	$\omega_n = 2.75$ eV, $\kappa = 1.03 \times 10^{-2}$ eV$\mathring{A}^{-2}$			$\omega_n = 3.1$ eV, $\kappa = 1.34 \times 10^{-2}$ eV$\mathring{A}^{-2}$		
δ(eV)	0.	0.1	0.2	0.	0.1	0.2
Γ_e(eV)	8.8×10^{-2}	5.5×10^{-2}	3.8×10^{-2}	$12. \times 10^{-2}$	5.8×10^{-2}	$5. \times 10^{-2}$
τ_e (fs)	7.5	12.	17.4	5.5	11.4	13.2

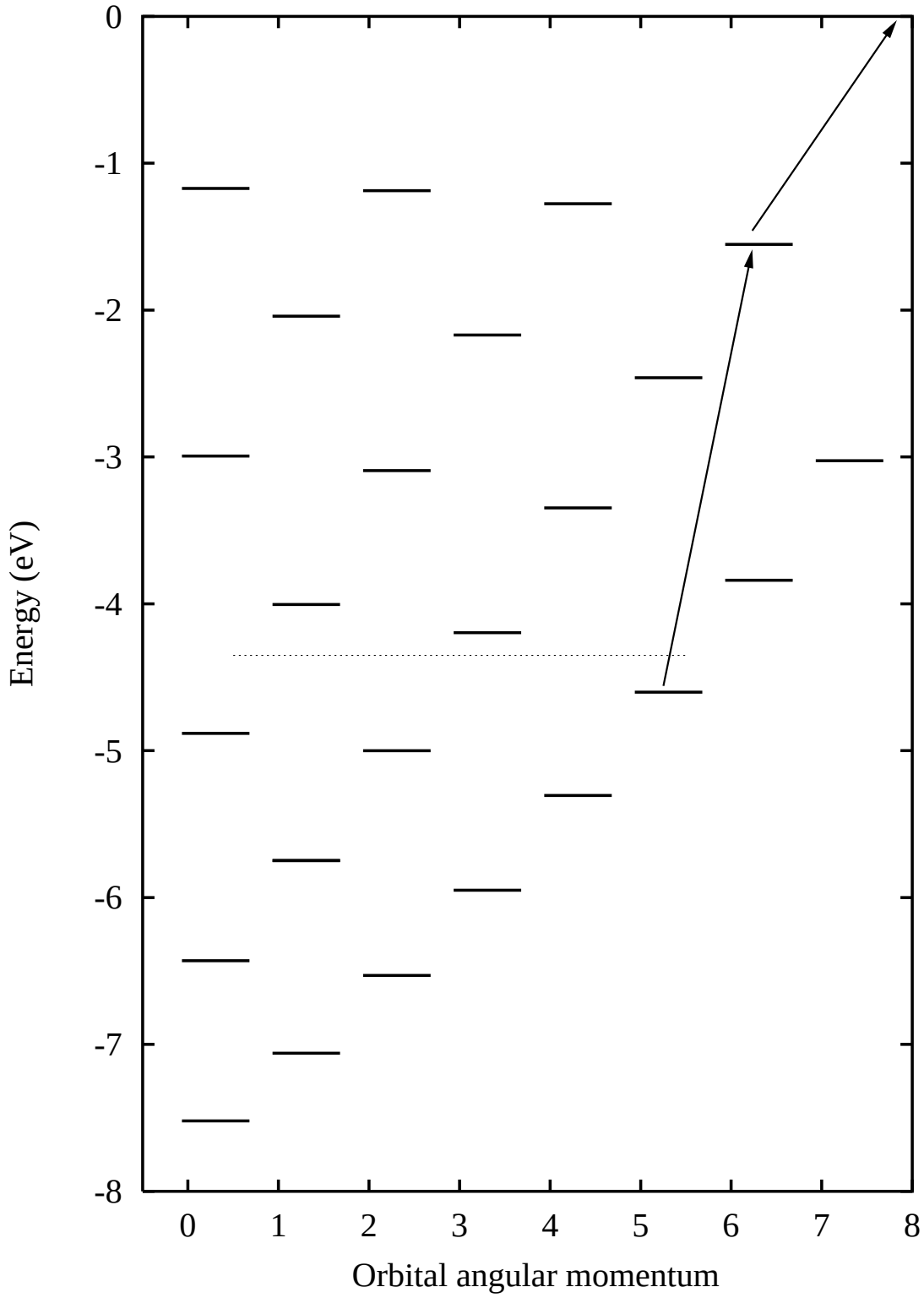
0
-1
-2
-3
-4
-5
-6
-7
-8
Energy (eV)
0
1
2
3
4
5
6
7
8
Orbital angular momentum

FIG. 1. Single-particle levels in the jellium model of Na_{93}^{+}. The Fermi level is indicated with a dotted line. The arrows show a two-step transition with a particularly small matrix element in eq. (16).

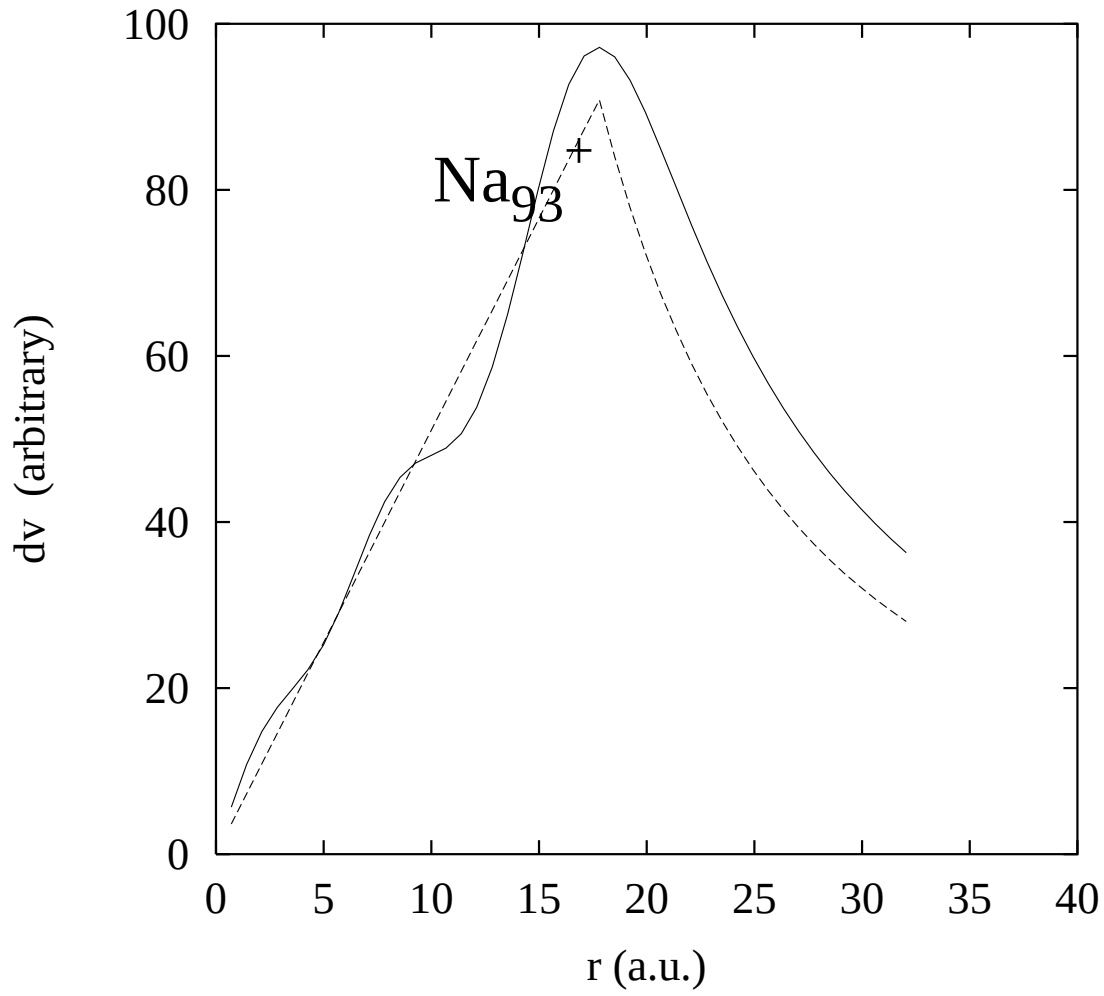

FIG. 2. Transition potential, comparing full RPA with eqs. (6,10)

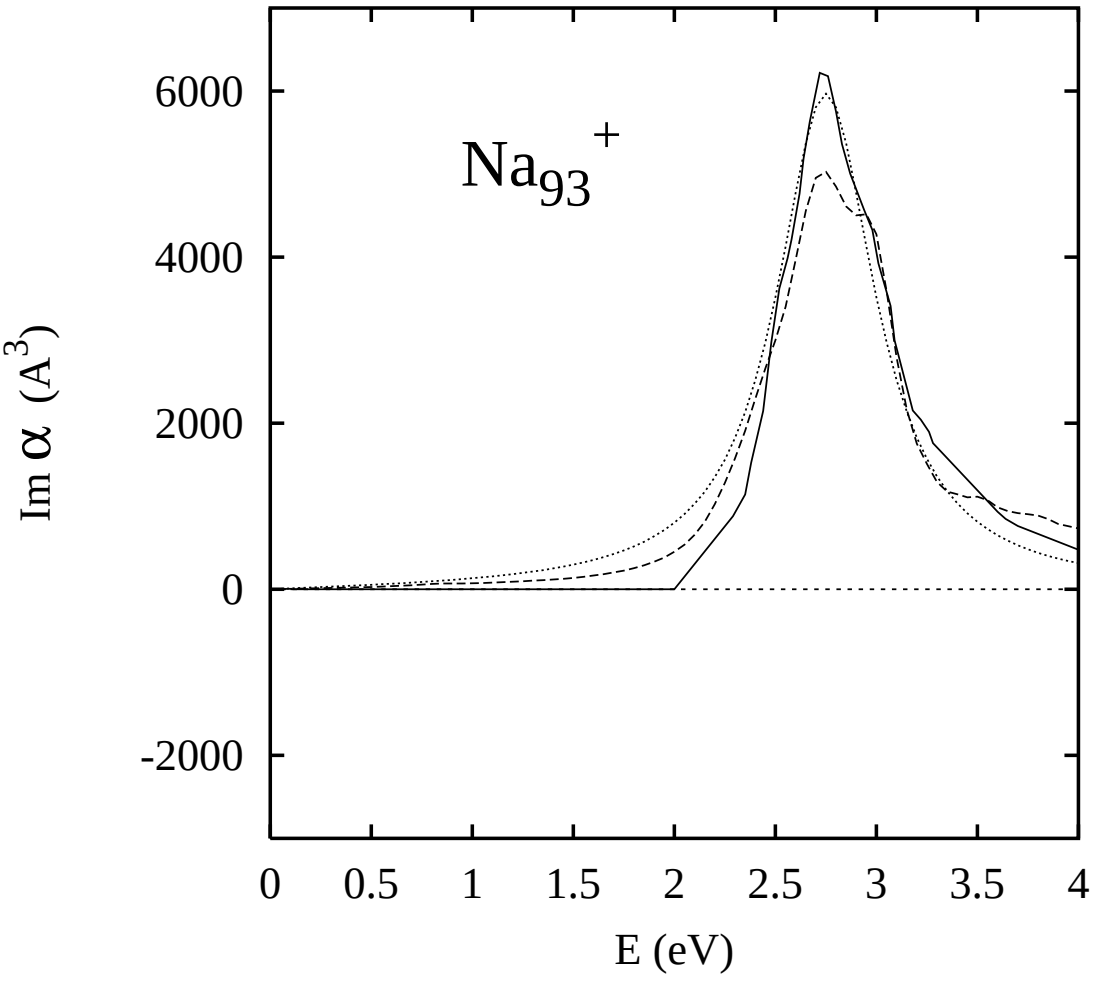

FIG. 3. Imaginary part of the dynamic polarizability of Na_{93}^{+}: empirical from ref. [2] and eq. (12) (solid line); single-pole approximation (dashed line); RPA with soft jellium model (dotted line).

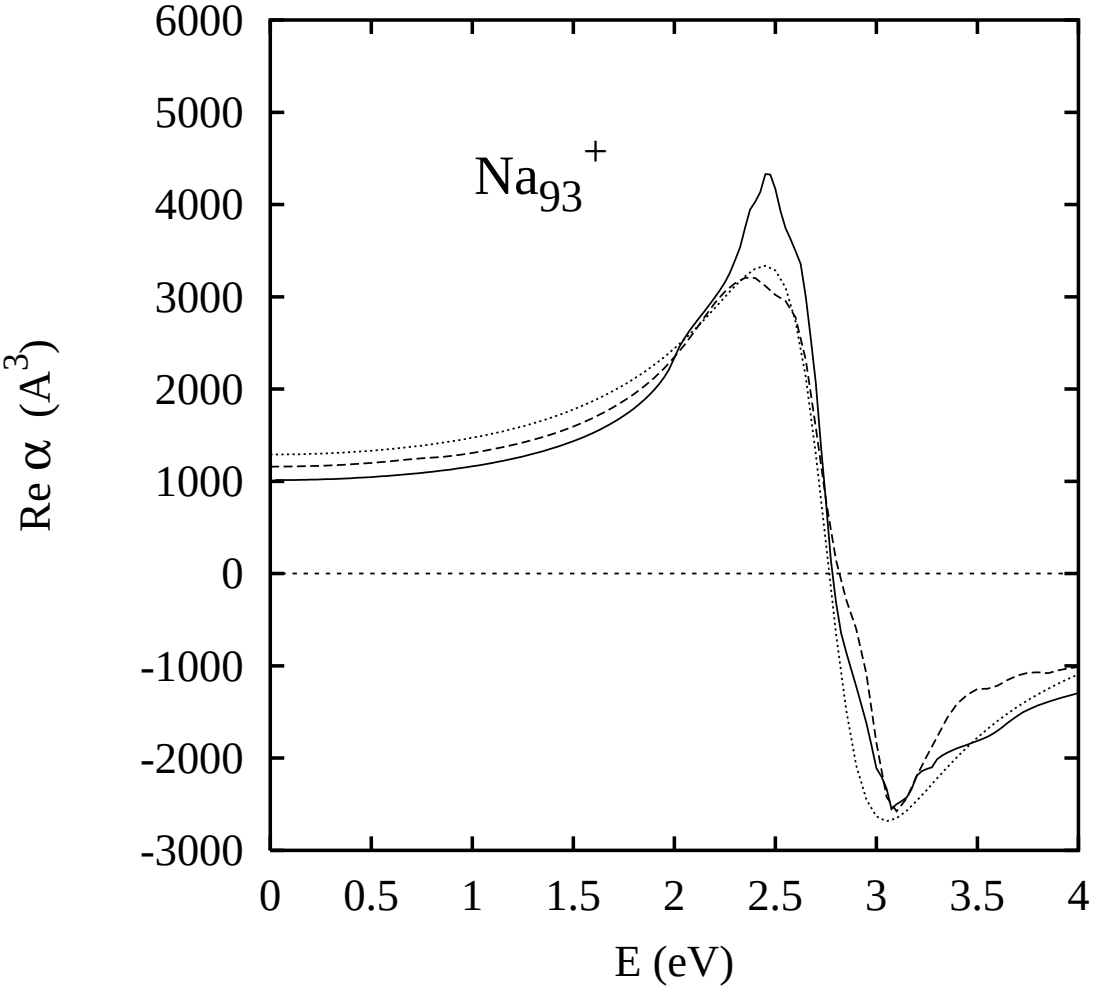

FIG. 4. Real part of the dynamic polarizability for Na_{93}^{+}. Empirical from Kramers-Kronig relation eq. (13), solid line; single-pole approximation (dashed line); RPA with soft jellium model (dotted line).

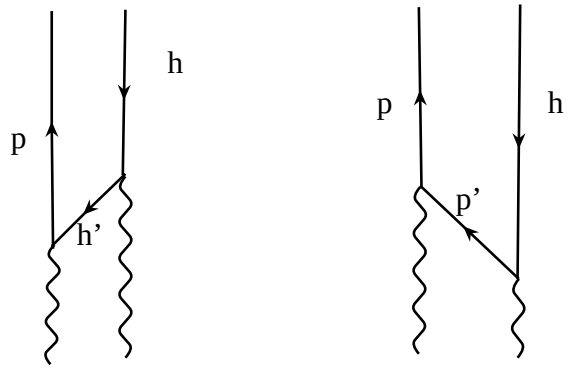

FIG. 5. Perturbation theory graphs for second-order ionization.

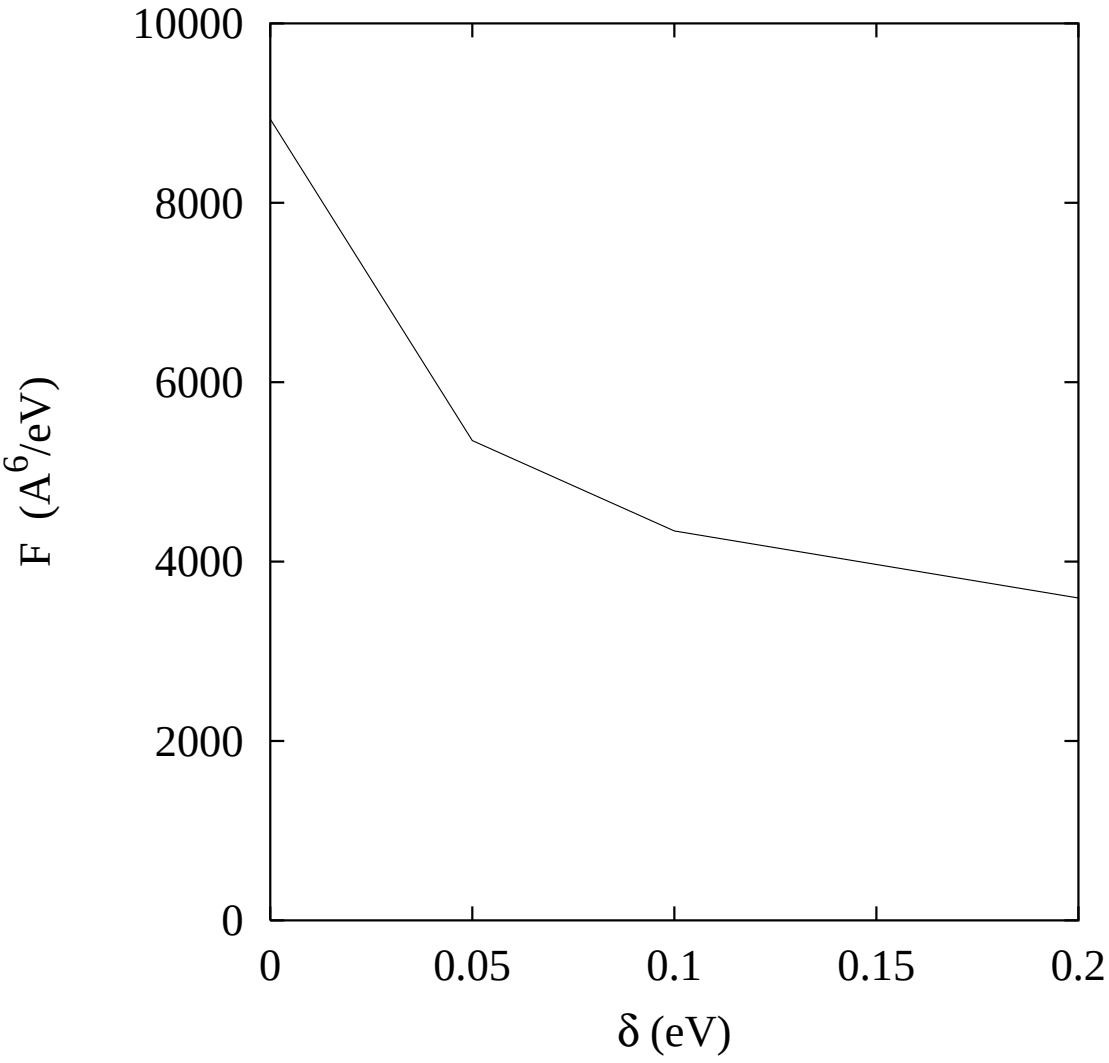

FIG. 6. Second-order term $\pi e^4/2|K^{(2)}|^2 dn_f/dE$ as a function of δ.